

SO₂ Poisoning of Cu-CHA deNO_x Catalyst: The Most Vulnerable Cu Species Identified by X-ray Absorption Spectroscopy

Anastasia Yu. Molokova, Elisa Borfecchia, Andrea Martini, Ilia A. Pankin, Cesare Atzori, Olivier Mathon, Silvia Bordiga, Fei Wen, Peter N. R. Vennestrøm, Gloria Berlier, Ton V. W. Janssens,* and Kirill A. Lomachenko*



Cite This: *JACS Au* 2022, 2, 787–792



Read Online

ACCESS |



Metrics & More



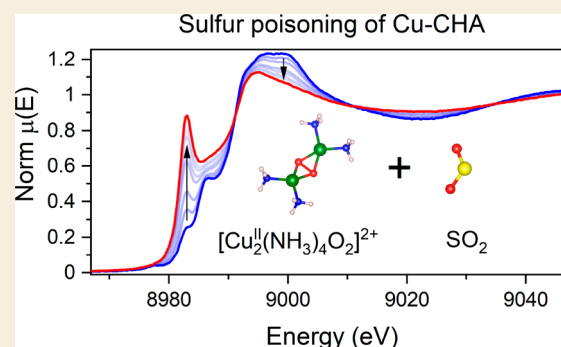
Article Recommendations



Supporting Information

ABSTRACT: Cu-exchanged chabazite zeolites (Cu-CHA) are effective catalysts for the NH₃-assisted selective catalytic reduction of NO (NH₃-SCR) for the abatement of NO_x emission from diesel vehicles. However, the presence of a small amount of SO₂ in diesel exhaust gases leads to a severe reduction in the low-temperature activity of these catalysts. To shed light on the nature of such deactivation, we characterized a Cu-CHA catalyst under well-defined exposures to SO₂ using *in situ* X-ray absorption spectroscopy. By varying the pretreatment procedure prior to the SO₂ exposure, we have selectively prepared Cu^I and Cu^{II} species with different ligations, which are relevant for the NH₃-SCR reaction. The highest reactivity toward SO₂ was observed for Cu^{II} species coordinated to both NH₃ and extraframework oxygen, in particular for [Cu^{II}₂(NH₃)₄O₂]²⁺ complexes. Cu species without either ammonia or extraframework oxygen ligands were much less reactive, and the associated SO₂ uptake was significantly lower. These results explain why SO₂ mostly affects the low-temperature activity of Cu-CHA catalysts, since the dimeric complex [Cu^{II}₂(NH₃)₄O₂]²⁺ is a crucial intermediate in the low-temperature NH₃-SCR catalytic cycle.

KEYWORDS: selective catalytic reduction, Cu-CHA, deNO_x catalysis, sulfur poisoning, X-ray absorption spectroscopy, X-ray adsorbate quantification, XAS, XAQ



The emission of nitrogen oxides (NO_x) from diesel vehicles is a global environmental challenge.^{1,2} State of the art exhaust gas aftertreatment systems contain catalysts for selective catalytic reduction of NO_x by ammonia (NH₃-SCR), capable of reducing well over 90% of the NO_x emitted by the engine. In the NH₃-SCR reaction, NO reacts with NH₃ in the presence of O₂ to form N₂ and H₂O. At present, Cu-exchanged chabazites (Cu-CHA) are the preferred catalysts for NH₃-SCR, due to their superior low-temperature activity (150–350 °C)^{3,4} and hydrothermal stability.^{5,6} The temperature dependence of the NH₃-SCR activity of Cu-CHA catalysts shows a minimum at around 350 °C, which indicates that the reaction mechanism at low temperatures is different from that at higher temperatures.⁷

The NH₃-SCR reaction cycle for the low-temperature activity is a redox cycle, consisting of a series of oxidation and reduction steps, in which the oxidation state of Cu changes between Cu^I and Cu^{II}. The NO and NH₃ coordinate to Cu in the zeolite, giving rise to a variety of Cu species along the NH₃-SCR cycle.^{8–11} The low-temperature activity of Cu-CHA catalysts originates from the ability to form mobile Cu^I(NH₃)₂ complexes under SCR conditions. Pairs of these species constitute the active Cu sites capable of O₂ activation via the

formation of [Cu^{II}₂(NH₃)₄O₂]²⁺ dimers around 200 °C, which is a crucial step in the NH₃-SCR reaction cycle.^{12,13}

In practice, the application of Cu-CHA catalysts for the NH₃-SCR is restricted to ultralow-sulfur diesel fuels, due to the fact that a few ppm of SO₂ present in the exhaust gas drastically reduces the activity at low temperatures.^{3,4,14} Multiple studies show that SO₂ affects the Cu mobility, the amount of Cu active sites,¹⁴ and the redox behavior of the Cu in the NH₃-SCR cycle.^{9,15} Most studies have focused on the overall effect of SO₂ on the performance of the catalysts,^{14–21} while the chemistry behind SO₂ poisoning at the molecular level remains poorly understood. To determine a mechanism for SO₂ poisoning, one must identify the species in the Cu-CHA catalysts that interact with SO₂. To this end, we have selectively prepared well-defined Cu^I and Cu^{II} species with

Received: January 27, 2022

Revised: April 4, 2022

Accepted: April 5, 2022

Published: April 11, 2022



Table 1. Pretreatment Procedures and Resulting Cu Species

procedure	conditions	dominant Cu state	designation in the text and figures	ref
1	1% H ₂ at 400 °C; cooling to 200 °C in He	fw-Cu ^I	fw-Cu ^I	24
2	500 ppm of NO + 600 ppm of NH ₃ at 200 °C	mobile [Cu ^I (NH ₃) ₂] ⁺	[Cu ^I (NH ₃) ₂] ⁺	24
3	500 ppm of NO + 600 ppm of NH ₃ at 200 °C; heating to 550 °C in He; cooling back to 200 °C in He	fw-Cu ^I (after thermal treatment of [Cu ^I (NH ₃) ₂] ⁺)	[Cu ^I (NH ₃) ₂] ⁺ + T	24
4	10% O ₂ at 200 °C	fw-Cu ^{II}	fw-Cu ^{II}	25
5	500 ppm of NO + 600 ppm of NH ₃ at 200 °C; He purge; 10% O ₂ at 200 °C	mobile [Cu ^{II} ₂ (NH ₃) ₄ O ₂] ²⁺ dimer	[Cu ^{II} ₂ (NH ₃) ₄ O ₂] ²⁺	13
6	600 ppm of NH ₃ at 200 °C	mixed ^a	Cu ^{II} + NH ₃	this work

^aProcedure 6 results in a mixture of two NH₃-coordinated Cu species, as discussed further in the text.

different ligands inside the pores of the Cu-CHA catalyst and exposed them to SO₂ under well-defined conditions. We monitored the changes in the Cu K-edge X-ray absorption spectra (XAS) during the absorption of SO₂. This allowed us to determine the chemical state of the Cu that interacts with SO₂. The results were corroborated by X-ray emission spectroscopy (XES) and measurements of the SO₂ uptake using temperature-programmed desorption (TPD) of SO₂.

The Cu-CHA catalyst used in this study had a Si/Al ratio of 6.7 and a Cu loading of 3.2 wt % (Cu/Al = 0.24). The Cu K-edge XAS and Cu Kβ valence-to-core XES measurements were carried out at the BM23²² and ID26²³ beamlines of the European Synchrotron Radiation Facility (ESRF), respectively. Sample treatment protocols consisted of three distinct steps. First, all samples were heated to 550 °C in a 10% O₂/He flow, removing water and forming Cu^{II} species bound to the framework of the zeolite (fw-Cu^{II}). Then, the specific state of Cu was prepared, using one of the six different pretreatment procedures summarized in Table 1. Finally, the catalyst was exposed to 400 ppm SO₂/He flow at 200 °C for 3 h until no visible changes in the spectra occurred. Further experimental details are given in the Supporting Information.

The Cu species formed with the pretreatments differ in three aspects: (1) the oxidation state of Cu (Cu^I or Cu^{II}), (2) the coordination of the Cu (NH₃ or/and O), and (3) the interaction of the Cu with the framework (fw-coordinated or mobile species).

Figure 1 shows the evolution of Cu K-edge XANES and EXAFS spectra during the exposure of the pretreated Cu-CHA catalyst to 400 ppm SO₂/He flow at 200 °C. For all Cu^I species and fw-Cu^{II} species (procedures 1–4 in Table 1), only minor changes are observed upon SO₂ exposure, indicating that these species are not very reactive toward SO₂. In contrast, for Cu^{II} species in the presence of NH₃ (procedures 5 and 6) significant changes are observed in the spectra. In these cases, the exposure to SO₂ results in a pronounced increase of the XANES peak at 8983 eV, characteristic for linear Cu^I complexes,^{9,26,27} and a decrease in the intensity of the first shell in the EXAFS FT. This means that some of the Cu^{II} species are reduced to Cu^I upon interaction with SO₂. The decrease in the first-shell intensity indicates a reduction of the coordination number for the Cu ions, which is also in line with the formation of a linear Cu^I species.

The species obtained in procedure 5 are the oxygen-bridged diamine dicopper complexes [Cu^{II}₂(NH₃)₄O₂]²⁺, which are formed by the reaction of O₂ with a pair of [Cu^I(NH₃)₂]⁺ complexes.¹³ In the reaction cycle for the low-temperature NH₃-SCR reaction,^{11,13,28} the [Cu^{II}₂(NH₃)₄O₂]²⁺ complexes react with NO, which eventually leads to the production of N₂

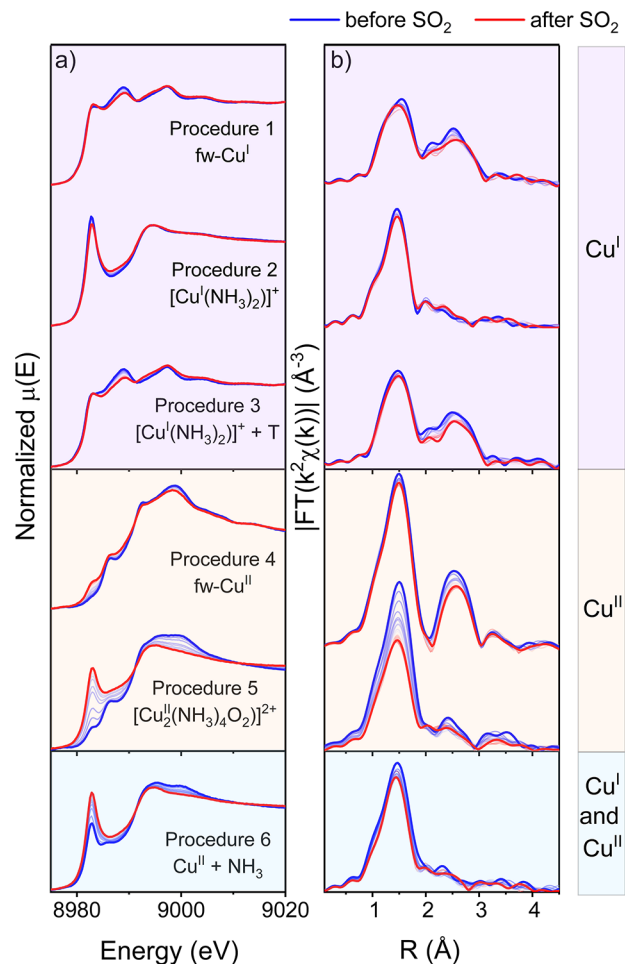


Figure 1. Cu K-edge XANES (a) and FT-EXAFS spectra (b) collected *in situ* during the exposure of Cu species obtained in procedures 1–6 to SO₂ at 200 °C.

and H₂O. The observation that the [Cu^{II}₂(NH₃)₄O₂]²⁺ complexes are reactive toward SO₂ is therefore a good explanation for the SO₂-induced deactivation of Cu-CHA catalysts for NH₃-SCR: the reaction with SO₂ interrupts the NH₃-SCR cycle, thereby decreasing the activity of the catalyst.

The other case where Cu reacts with SO₂ is obtained in procedure 6 by exposure of the fw-Cu^{II} species to NH₃. Previously, a similar pretreatment resulted in a mixture of linear [Cu^I(NH₃)₂]⁺ and either square-planar [Cu^{II}(NH₃)₄]²⁺ complexes or mixed-ligand [Cu^{II}O_x(NH₃)_y]²⁺ moieties.^{9,24} For the sample reported in this work, the mixed-ligand configuration is more likely. Indeed, linear combination fits

of the XANES data on the basis of references for the linear $[\text{Cu}^{\text{I}}(\text{NH}_3)_2]^+$ complex and pure $\text{Cu}^{\text{II}}(\text{NH}_3)_4$ groups (aqueous $[\text{Cu}^{\text{II}}(\text{NH}_3)_4]^{2+}$ or solid-state $[\text{Cu}^{\text{II}}(\text{NH}_3)_4]\text{SO}_4 \cdot \text{H}_2\text{O}$) resulted in visible discrepancies with the data (Figure S7 in the Supporting Information). A better agreement is obtained when the spectrum of oxygen-bridged diamine dicopper complex $[\text{Cu}^{\text{II}}_2(\text{NH}_3)_4\text{O}_2]^{2+}$ is used as a Cu^{II} reference in combination with $[\text{Cu}^{\text{I}}(\text{NH}_3)_2]^+$, with approximately equal weights for each component (Figure 2). The necessary stock of available oxygen

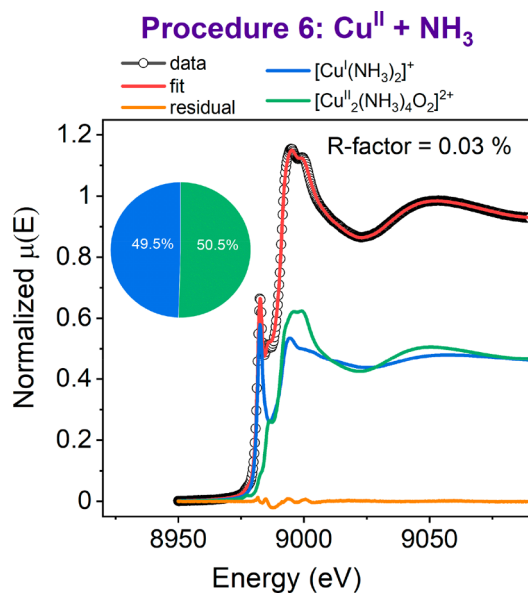


Figure 2. Linear combination fit of Cu K-edge XANES spectra obtained in Cu-CHA after exposing fw- Cu^{II} species to NH_3 at 200 °C ($\text{Cu}^{\text{II}} + \text{NH}_3$ pretreatment).

needed for the formation of the mixed-ligand species is expected to be present in the sample, as a wavelet analysis of the EXAFS collected after heating to 550 °C and cooling to 200 °C in 10% O_2/He flow reveals the presence of Cu–Cu scattering usually attributed to the oxygen-containing dimers^{29,30} (Figure S8 in the Supporting Information), which may be susceptible to form mixed-ligand species upon exposure to NH_3 .

The evolution of XANES spectra upon interaction with SO_2 shows that the most susceptible species are Cu^{II} with mixed $(\text{NH}_3)_x\text{O}_y$ ligation, whereas Cu^{I} species or Cu^{II} in the absence of NH_3 are much less affected. These findings are supported by X-ray adsorbate quantification (XAQ) data,³¹ collected simultaneously with the XAS measurements during the exposure to SO_2 , and a TPD analysis of a parallel set of catalyst samples, exposed to the same pretreatments used in XANES experiments (Figure 3a). We find the highest sulfur content (S/Cu ratio) for the $[\text{Cu}^{\text{II}}_2(\text{NH}_3)_4\text{O}_2]^{2+}$ and $\text{Cu}^{\text{II}} + \text{NH}_3$ procedures. The sulfur uptake of the $[\text{Cu}^{\text{I}}(\text{NH}_3)_2]^+$ and fw- Cu^{II} moieties was ca. 3 times lower, and for the bare fw- Cu^{I} species, it was ca. 6 times lower. These results show that the reaction between the $[\text{Cu}^{\text{II}}_2(\text{NH}_3)_4\text{O}_2]^{2+}$ species and SO_2 contributes the most to the accumulation of SO_2 in the Cu-CHA catalyst.

Interestingly, the sulfur content in the $\text{Cu}^{\text{II}} + \text{NH}_3$ sample lies between those for samples with pure $[\text{Cu}^{\text{I}}(\text{NH}_3)_2]^+$ and $[\text{Cu}^{\text{II}}_2(\text{NH}_3)_4\text{O}_2]^{2+}$ species, which in combination with the linear combination fit shown in Figure 2 suggests that the

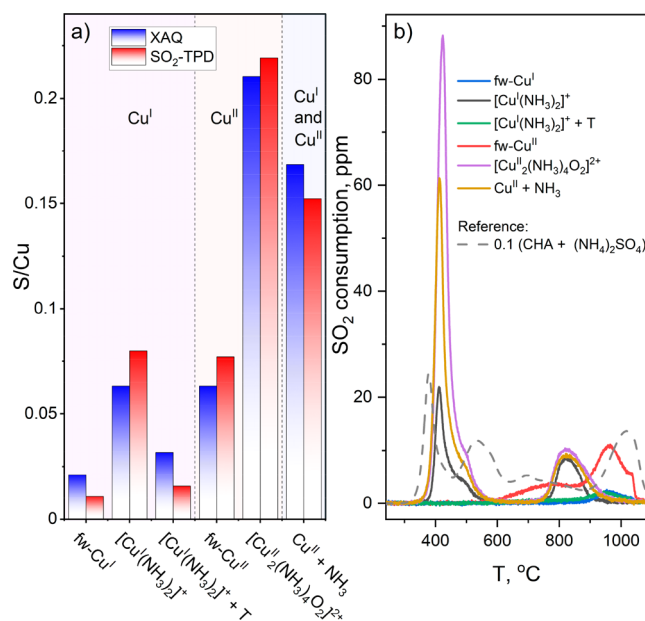


Figure 3. (a) S/Cu ratios in the samples after exposure to SO_2 obtained from SO_2 -TPD and XAQ. (b) SO_2 -TPD profiles collected after exposure of the species obtained in procedures 1–6 to SO_2 in comparison to a reference SO_2 -TPD curve of a CHA zeolite without Cu impregnated with 20 wt % $(\text{NH}_4)_2\text{SO}_4$, downscaled $\times 10$.

reactivity of the $\text{Cu}^{\text{II}}(\text{NH}_3)_x\text{O}_y$ species obtained after $\text{Cu}^{\text{II}} + \text{NH}_3$ treatment toward SO_2 is similar to that of $[\text{Cu}^{\text{II}}_2(\text{NH}_3)_4\text{O}_2]^{2+}$.

By comparing the SO_2 -TPD curves of Cu-CHA samples with that of $(\text{NH}_4)_2\text{SO}_4$ adsorbed on Cu-free CHA (Figure 3b), we can also deduce that the elevated sulfur content in the samples with the $\text{Cu}^{\text{II}}(\text{NH}_3)_x\text{O}_y$ species is due to the reactivity toward SO_2 and not to the formation of $(\text{NH}_4)_2\text{SO}_4$ in a reaction of SO_2 with NH_3 and NH_4^+ groups stored in the zeolite framework. For the adsorbed $(\text{NH}_4)_2\text{SO}_4$, we observe SO_2 desorption at around 380, 530, and 1000 °C (gray curve in Figure 3b). The desorption at 380 °C matches the known thermal decomposition of $(\text{NH}_4)_2\text{SO}_4$,³² the other two peaks are probably due to the interaction of either $(\text{NH}_4)_2\text{SO}_4$ or products of its decomposition with the zeolite, their precise interpretation being beyond the scope of the present argument. For all three Cu-CHA samples containing NH_3 before exposure to SO_2 ($[\text{Cu}^{\text{I}}(\text{NH}_3)_2]^+$, $[\text{Cu}^{\text{II}}_2(\text{NH}_3)_4\text{O}_2]^{2+}$, and $(\text{Cu}^{\text{II}} + \text{NH}_3)$ procedures), we observe SO_2 desorption at around 420 °C (Figure 3b). As this does not match any of the observed desorption characteristics of $(\text{NH}_4)_2\text{SO}_4$ in Cu-free Cu-CHA, the SO_2 -TPD feature at 420 °C reflects an interaction of Cu with SO_2 . Interestingly, the SO_2 -TPD curve for the sample with the dominant fw- Cu^{II} species shows a significant SO_2 desorption peak close to 1000 °C, which, together with the lack of changes in Cu K-edge XANES upon exposure to SO_2 , indicates the formation of some sulfur deposits not directly coordinated to Cu.

The presence of Cu–N and Cu–O bonds in the $[\text{Cu}^{\text{II}}_2(\text{NH}_3)_4\text{O}_2]^{2+}$ complex has been independently confirmed by valence-to-core XES.^{27,33,34} XES spectra at different stages of pretreatment leading to the formation of $[\text{Cu}^{\text{II}}_2(\text{NH}_3)_4\text{O}_2]^{2+}$ dimers are reported in Figure 4. The origin of the $K\beta'$ satellite peak is the transition from the ligand s orbitals to Cu 1s, which makes its position sensitive to the species directly coordinated to Cu and allows it to discriminate

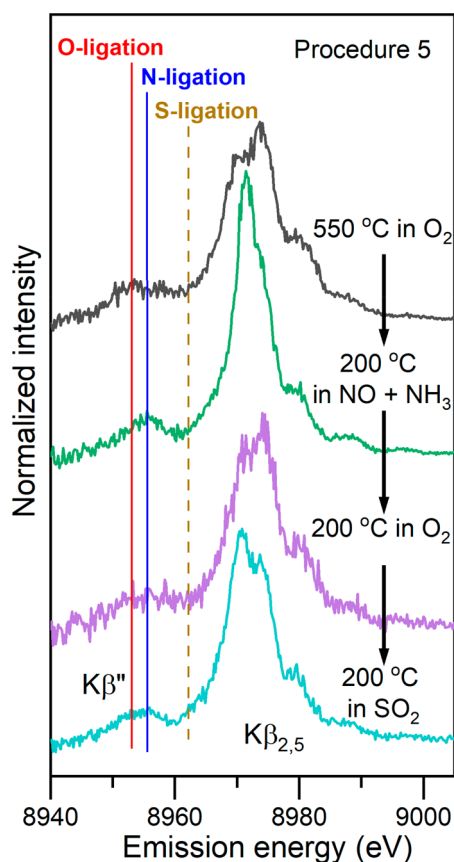


Figure 4. Background-subtracted Cu $K\beta$ valence-to-core XES spectra for different stages of procedure 5 leading to the formation of the $[\text{Cu}^{\text{II}}_2(\text{NH}_3)_4\text{O}_2]^{2+}$ complex and its exposure to SO_2 .

among Cu–O, Cu–N, and Cu–S bonds.^{35–37} Figure 4 shows that after heating in O_2 Cu is predominantly coordinated by oxygens (as expected for the fw- Cu^{II} species), whereas after exposure to $\text{NO} + \text{NH}_3$ N ligands are dominating, as expected for a $[\text{Cu}^{\text{I}}(\text{NH}_3)_2]^+$ linear complex. After subsequent exposure to O_2 and formation of $[\text{Cu}^{\text{II}}_2(\text{NH}_3)_4\text{O}_2]^{2+}$ dimers, the peak broadens, confirming the presence of both Cu–N and Cu–O bonds. These bonds remain after exposure to SO_2 , while no significant contribution from Cu–S bonds³⁸ is observed, suggesting that the possible SO_2 binding to the Cu is carried out through an oxygen atom.

In conclusion, the *in situ* XAS and XES measurements of different Cu intermediates formed in a Cu-CHA catalyst exposed to SO_2 demonstrate that Cu^{II} species with mixed NH_3 and O ligation of Cu are particularly reactive toward SO_2 , whereas Cu^{I} species and Cu^{II} without NH_3 are much less affected by it. In particular, the $[\text{Cu}^{\text{II}}_2(\text{NH}_3)_4\text{O}_2]^{2+}$ complex, which is formed upon activation of O_2 in the NH_3 -SCR cycle, shows a clear reaction with SO_2 , resulting in a partial reduction of the Cu^{II} and accumulation of sulfur in the zeolite. Therefore, we conclude that this reaction is responsible for the poisoning of Cu-CHA catalysts in NH_3 -SCR by SO_2 .

ASSOCIATED CONTENT

Supporting Information

The Supporting Information is available free of charge at <https://pubs.acs.org/doi/10.1021/jacsau.2c00053>.

Experimental details, XANES linear combination fits before SO_2 exposure, wavelet transform analysis of the sample heated in O_2 , and EXAFS fitting results (PDF)

AUTHOR INFORMATION

Corresponding Authors

Kirill A. Lomachenko – European Synchrotron Radiation Facility, 38043 Grenoble Cedex 9, France; orcid.org/0000-0003-0238-1719; Email: lomachenko@esrf.fr

Ton V. W. Janssens – Umicore Denmark ApS, 2970 Hørsholm, Denmark; orcid.org/0000-0002-1225-0942; Email: tonv.w.janssens@eu.umicore.com

Authors

Anastasia Yu. Molokova – European Synchrotron Radiation Facility, 38043 Grenoble Cedex 9, France; Department of Chemistry and NIS Centre, University of Turin, 10125 Turin, Italy; orcid.org/0000-0003-2053-2031

Elisa Borfecchia – Department of Chemistry and NIS Centre, University of Turin, 10125 Turin, Italy; orcid.org/0000-0001-8374-8329

Andrea Martini – Department of Chemistry and NIS Centre, University of Turin, 10125 Turin, Italy; The Smart Materials Research Institute, Southern Federal University, 344090 Rostov-on-Don, Russia; orcid.org/0000-0001-8820-2157

Ilia A. Pankin – The Smart Materials Research Institute, Southern Federal University, 344090 Rostov-on-Don, Russia

Cesare Atzori – European Synchrotron Radiation Facility, 38043 Grenoble Cedex 9, France; orcid.org/0000-0002-3227-7421

Olivier Mathon – European Synchrotron Radiation Facility, 38043 Grenoble Cedex 9, France

Silvia Bordiga – Department of Chemistry and NIS Centre, University of Turin, 10125 Turin, Italy; orcid.org/0000-0003-2371-4156

Fei Wen – Umicore AG & Co, 63457 Hanau, Germany

Peter N. R. Vennestrom – Umicore Denmark ApS, 2970 Hørsholm, Denmark; orcid.org/0000-0002-6744-5640

Gloria Berlier – Department of Chemistry and NIS Centre, University of Turin, 10125 Turin, Italy; orcid.org/0000-0001-7720-3584

Complete contact information is available at: <https://pubs.acs.org/10.1021/jacsau.2c00053>

Funding

This project has received funding from the European Union's Horizon 2020 research and innovation programme under the Marie Skłodowska-Curie grant agreement No. 847439.

Notes

The authors declare no competing financial interest.

ACKNOWLEDGMENTS

ESRF is kindly acknowledged for the provision of beamtime at the BM23 and ID26 beamlines. We thank N. Daffé and B. Detlefs for help during the XES experiment at ID26.

REFERENCES

- (1) Lambert, C. K. Perspective on SCR NO_x control for diesel vehicles. *React. Chem. Eng.* **2019**, *4* (6), 969–974.
- (2) Gounder, R.; Moini, A. Automotive NO_x abatement using zeolite-based technologies. *React. Chem. Eng.* **2019**, *4* (6), 966–968.

- (3) Hammershoi, P. S.; Jensen, A. D.; Janssens, T. V. W. Impact of SO_2 -poisoning over the lifetime of a Cu-CHA catalyst for NH_3 -SCR. *Appl. Catal., B* **2018**, *238*, 104–110.
- (4) Hammershoi, P. S.; Jangjou, Y.; Epling, W. S.; Jensen, A. D.; Janssens, T. V. W. Reversible and irreversible deactivation of Cu-CHA NH_3 -SCR catalysts by SO_2 and SO_3 . *Appl. Catal., B* **2018**, *226*, 38–45.
- (5) Peden, C. H. F. Cu/Chabazite catalysts for 'Lean-Burn' vehicle emission control. *J. Catal.* **2019**, *373*, 384–389.
- (6) Borfecchia, E.; Lomachenko, K. A.; Giordanino, F.; Falsig, H.; Beato, P.; Soldatov, A. V.; Bordiga, S.; Lamberti, C. Revisiting the nature of Cu-sites in activated Cu-SSZ-13 catalyst for SCR reaction. *Chem. Sci.* **2015**, *6*, 548–563.
- (7) Gao, F.; Walter, E. D.; Kollar, M.; Wang, Y.; Szanyi, J.; Peden, C. H. F. Understanding ammonia selective catalytic reduction kinetics over Cu/SSZ-13 from motion of the Cu ions. *J. Catal.* **2014**, *319*, 1–14.
- (8) Feng, Y.; Wang, X.; Janssens, T. V. W.; Vennestrom, P. N. R.; Jansson, J.; Skoglundh, M.; Grönbeck, H. First-Principles Microkinetic Model for Low-Temperature NH_3 -Assisted Selective Catalytic Reduction of NO over Cu-CHA. *ACS Catal.* **2021**, *11*, 14395–14407.
- (9) Janssens, T. V. W.; Falsig, H.; Lundegaard, L. F.; Vennestrom, P. N. R.; Rasmussen, S. B.; Moses, P. G.; Giordanino, F.; Borfecchia, E.; Lomachenko, K. A.; Lamberti, C.; Bordiga, S.; Godiksen, A.; Mossin, S.; Beato, P. A Consistent Reaction Scheme for the Selective Catalytic Reduction of Nitrogen Oxides with Ammonia. *ACS Catal.* **2015**, *5* (5), 2832–2845.
- (10) Gao, F.; Mei, D.; Wang, Y.; Szanyi, J.; Peden, C. H. Selective Catalytic Reduction over Cu/SSZ-13: Linking Homo- and Heterogeneous Catalysis. *J. Am. Chem. Soc.* **2017**, *139* (13), 4935–4942.
- (11) Paolucci, C.; Khurana, I.; Parekh, A. A.; Li, S. C.; Shih, A. J.; Li, H.; Di Iorio, J. R.; Albarracin-Caballero, J. D.; Yezerets, A.; Miller, J. T.; Delgass, W. N.; Ribeiro, F. H.; Schneider, W. F.; Gounder, R. Dynamic multinuclear sites formed by mobilized copper ions in NO_x selective catalytic reduction. *Science* **2017**, *357* (6354), 898–903.
- (12) Jones, C. B.; Khurana, I.; Krishna, S. H.; Shih, A. J.; Delgass, W. N.; Miller, J. T.; Ribeiro, F. H.; Schneider, W. F.; Gounder, R. Effects of dioxygen pressure on rates of NO_x selective catalytic reduction with NH_3 on Cu-CHA zeolites. *J. Catal.* **2020**, *389*, 140–149.
- (13) Negri, C.; Selli, T.; Borfecchia, E.; Martini, A.; Lomachenko, K. A.; Janssens, T. V. W.; Cutini, M.; Bordiga, S.; Berlier, G. Structure and Reactivity of Oxygen-Bridged Diamino Dicopper(II) Complexes in Cu-Ion-Exchanged Chabazite Catalyst for NH_3 -Mediated Selective Catalytic Reduction. *J. Am. Chem. Soc.* **2020**, *142* (37), 15884–15896.
- (14) Tang, Y. D.; Wang, D.; Wang, X.; Zha, Y. H.; An, H. M.; Kamasamudram, K.; Yezerets, A. Impact of low temperature sulfur exposure on the aging of small pore Cu-zeolite SCR catalyst. *Catal.* **2021**, *360*, 234–240.
- (15) Mesilov, V. V.; Bergman, S. L.; Dahlin, S.; Yang, X.; Xi, S. B.; Ma, Z. R.; Lian, X.; Wei, C.; Pettersson, L. J.; Bernasek, S. L. Differences in oxidation-reduction kinetics and mobility of Cu species in fresh and SO_2 -poisoned Cu-SSZ-13 catalysts. *Appl. Catal., B* **2021**, *284*, 119756.
- (16) Mesilov, V.; Xiao, Y.; Dahlin, S.; Bergman, S. L.; Pettersson, L. J.; Bernasek, S. L. First-Principles Calculations of Condition-Dependent Cu/Fe Speciation in Sulfur-Poisoned Cu- and Fe-SSZ-13 Catalysts. *J. Phys. Chem. C* **2021**, *125* (8), 4632–4645.
- (17) Feng, Y.; Janssens, T. V. W.; Vennestrom, P. N. R.; Jansson, J.; Skoglundh, M.; Grönbeck, H. The Role of H^+ - and Cu^+ -Sites for N_2O Formation during NH_3 -SCR over Cu-CHA. *J. Phys. Chem. C* **2021**, *125* (8), 4595–4601.
- (18) Millan, R.; Cnudde, P.; van Speybroeck, V.; Boronat, M. Mobility and Reactivity of Cu^+ Species in Cu-CHA Catalysts under NH_3 -SCR- NO_x Reaction Conditions: Insights from AIMD Simulations. *JACS Au* **2021**, *1* (10), 1778–1787.
- (19) Krishna, S. H.; Jones, C. B.; Gounder, R. Temperature dependence of Cu(I) oxidation and Cu(II) reduction kinetics in the selective catalytic reduction of NO_x with NH_3 on Cu-chabazite zeolites. *J. Catal.* **2021**, *404*, 873–882.
- (20) Mesilov, V. V.; Dahlin, S.; Bergman, S. L.; Xi, S.; Han, J.; Olsson, L.; Pettersson, L. J.; Bernasek, S. L. Regeneration of sulfur-poisoned Cu-SSZ-13 catalysts: Copper speciation and catalytic performance evaluation. *Appl. Catal., B* **2021**, *299*, 120626.
- (21) Negri, C.; Borfecchia, E.; Martini, A.; Deplano, G.; Lomachenko, K. A.; Janssens, T. V. W.; Berlier, G.; Bordiga, S. In situ X-ray absorption study of Cu species in Cu-CHA catalysts for NH_3 -SCR during temperature-programmed reduction in NO/NH_3 . *Rev. Chem. Intermed.* **2021**, *47* (1), 357–375.
- (22) Mathon, O.; Beteva, A.; Borrel, J.; Bugnazet, D.; Gatla, S.; Hino, R.; Kantor, I.; Mairs, T.; Munoz, M.; Pasternak, S.; Perrin, F.; Pascarelli, S. The time-resolved and extreme conditions XAS (TEXAS) facility at the European Synchrotron Radiation Facility: the general-purpose EXAFS bending-magnet beamline BM23. *J. Synchrotron Radiat.* **2015**, *22* (6), 1548–1554.
- (23) Glatzel, P.; Harris, A.; Marion, P.; Sikora, M.; Weng, T. C.; Guilloud, C.; Lafuerza, S.; Rovezzi, M.; Detlefs, B.; Ducotte, L. The five-analyzer point-to-point scanning crystal spectrometer at ESRF ID26. *J. Synchrotron Radiat.* **2021**, *28*, 362–371.
- (24) Borfecchia, E.; Negri, C.; Lomachenko, K. A.; Lamberti, C.; Janssens, T. V. W.; Berlier, G. Temperature-dependent dynamics of NH_3 -derived Cu species in the Cu-CHA SCR catalyst. *React. Chem. Eng.* **2019**, *4* (6), 1067–1080.
- (25) Martini, A.; Borfecchia, E.; Lomachenko, K. A.; Pankin, I. A.; Negri, C.; Berlier, G.; Beato, P.; Falsig, H.; Bordiga, S.; Lamberti, C. Composition-driven Cu-speciation and reducibility in Cu-CHA zeolite catalysts: a multivariate XAS/FTIR approach to complexity. *Chem. Sci.* **2017**, *8* (10), 6836–6851.
- (26) Kau, L. S.; Spira-Solomon, D. J.; Penner-Hahn, J. E.; Hodgson, K. O.; Solomon, E. I. X-ray absorption edge determination of the oxidation state and coordination number of copper. Application to the type 3 site in Rhus vernicifera laccase and its reaction with oxygen. *J. Am. Chem. Soc.* **1987**, *109* (21), 6433–6442.
- (27) Giordanino, F.; Borfecchia, E.; Lomachenko, K. A.; Lazzarini, A.; Agostini, G.; Gallo, E.; Soldatov, A. V.; Beato, P.; Bordiga, S.; Lamberti, C. Interaction of NH_3 with Cu-SSZ-13 Catalyst: A Complementary FTIR, XANES, and XES Study. *J. Phys. Chem. Lett.* **2014**, *5* (9), 1552–1559.
- (28) Chen, L.; Janssens, T. V. W.; Vennestrom, P. N. R.; Jansson, J.; Skoglundh, M.; Grönbeck, H. A Complete Multisite Reaction Mechanism for Low-Temperature NH_3 -SCR over Cu-CHA. *ACS Catal.* **2020**, *10* (10), 5646–5656.
- (29) Martini, A.; Signorile, M.; Negri, C.; Kvande, K.; Lomachenko, K. A.; Svelle, S.; Beato, P.; Berlier, G.; Borfecchia, E.; Bordiga, S. EXAFS wavelet transform analysis of Cu-MOR zeolites for the direct methane to methanol conversion. *Phys. Chem. Chem. Phys.* **2020**, *22* (34), 18950–18963.
- (30) Sushkevich, V. L.; Safonova, O. V.; Palagin, D.; Newton, M. A.; van Bokhoven, J. A. Structure of copper sites in zeolites examined by Fourier and wavelet transform analysis of EXAFS. *Chem. Sci.* **2020**, *11* (20), 5299–5312.
- (31) Lomachenko, K. A.; Molokova, A. Y.; Atzori, C.; Mathon, O. Quantification of Adsorbates by X-ray Absorption Spectroscopy: Getting TGA-like Information for Free. *J. Phys. Chem. C* **2022**, *126* (11), 5175–5179.
- (32) Kiyoura, R.; Urano, K. Mechanism, Kinetics, and Equilibrium of Thermal Decomposition of Ammonium Sulfate. *Ind. Eng. Chem. Process* **1970**, *9* (4), 489–494.
- (33) Gunter, T.; Carvalho, H. W. P.; Doronkin, D. E.; Sheppard, T.; Glatzel, P.; Atkins, A. J.; Rudolph, J.; Jacob, C. R.; Casapu, M.; Grunwaldt, J. D. Structural snapshots of the SCR reaction mechanism on Cu-SSZ-13. *Chem. Commun.* **2015**, *51* (44), 9227–9230.
- (34) Gunter, T.; Doronkin, D. E.; Boubnov, A.; Carvalho, H. W. P.; Casapu, M.; Grunwaldt, J. D. The SCR of NO_x with NH_3 Examined by Novel X-ray Emission and X-ray Absorption Methods. *Top. Catal.* **2016**, *59* (10–12), 866–874.
- (35) Lomachenko, K. A.; Borfecchia, E.; Negri, C.; Berlier, G.; Lamberti, C.; Beato, P.; Falsig, H.; Bordiga, S. The Cu-CHA de NO_x catalyst in action: temperature-dependent NH_3 -assisted selective

catalytic reduction monitored by operando XAS and XES. *J. Am. Chem. Soc.* **2016**, *138* (37), 12025–12028.

(36) Glatzel, P.; Bergmann, U. High resolution 1s core hole X-ray spectroscopy in 3d transition metal complexes - electronic and structural information. *Coord. Chem. Rev.* **2005**, *249* (1–2), 65–95.

(37) Vegelius, J. R.; Kvashnina, K. O.; Klintonberg, M.; Soroka, I. L.; Butorin, S. M. Cu $K\beta_{2,5}$ X-ray emission spectroscopy as a tool for characterization of monovalent copper compounds. *J. Anal. At. Spectrom.* **2012**, *27* (11), 1882–1888.

(38) Muller, P.; Neuba, A.; Florke, U.; Henkel, G.; Kuhne, T. D.; Bauer, M. Experimental and Theoretical High Energy Resolution Hard X-ray Absorption and Emission Spectroscopy on Biomimetic Cu_2S_2 Complexes. *J. Phys. Chem. A* **2019**, *123* (16), 3575–3581.

Recommended by ACS

Selective Catalytic Reduction of NO_x with NH_3 over Cu/SSZ-13: Elucidating Dynamics of Cu Active Sites with In Situ UV–Vis Spectroscopy and DFT Calculations

Yani Zhang, Feng Gao, *et al.*

MAY 12, 2022

THE JOURNAL OF PHYSICAL CHEMISTRY C

READ 

Influence of ZCuOH, Z₂Cu, and Extraframework Cu_xO_y Species in Cu-SSZ-13 on N_2O Formation during the Selective Catalytic Reduction of NO_x with NH_3

Arthur J. Shih, Aída Luz Villa, *et al.*

AUGUST 05, 2021

ACS CATALYSIS

READ 

Toward Rational Design of Cu/SSZ-13 Selective Catalytic Reduction Catalysts: Implications from Atomic-Level Understanding of Hydrothermal Stability

James Song, Feng Gao, *et al.*

OCTOBER 24, 2017

ACS CATALYSIS

READ 

Spectroscopic Evidence and Density Functional Theory (DFT) Analysis of Low-Temperature Oxidation of Cu⁺ to Cu²⁺+ NO_x in Cu-CHA Catalysts: Implications for t...

Marta Moreno-González, Mercedes Boronat, *et al.*

FEBRUARY 14, 2019

ACS CATALYSIS

READ 

Get More Suggestions >